Virologica Sinica 38 (2023) 222–232

Contents lists available at ScienceDirect

Virologica Sinica

journal homepage: www.keaipublishing.com/en/journals/virologica-sinica
www.virosin.org

Research Article

Splicing factor SF3B3, a NS5-binding protein, restricts ZIKV infection by targeting GCH1

Tanxiu Chen [a,b], Hao Yang [a], Penghui Liu [a], Moliduer Hamiti [c], Xintian Zhang [a], Yi Xu [a], Wenqi Quan [a], Yong Zhang [a], Wenhai Yu [a], Li Jiao [a], Tingfu Du [a], Juemin Xi [a], Bin Yin [c], Wei Zhou [b], Shuaiyao Lu [a,*], Xiaozhong Peng [a,c,*]

[a] *Institute of Medical Biology, Chinese Academy of Medical Sciences and Peking Union Medical College, Kunming, 650031, China*
[b] *Department of Science and Education, Jiangxi Key Laboratory of Translational Cancer Research, Jiangxi Cancer Hospital, Nanchang, 330029, China*
[c] *The State Key Laboratory of Medical Molecular Biology, Department of Molecular Biology and Biochemistry, Institute of Basic Medical Sciences, Medical Primate Research Center, Neuroscience Center, Chinese Academy of Medical Sciences and Peking Union Medical College, Beijing, 100730, China*

ARTICLE INFO

Keywords:
Nonstructural protein 5 (NS5)
Splicing factor 3b subunit 3 (SF3B3)
GTP cyclohydrolase I (GCH1)
IFN-stimulated gene (ISGs)
IFN signalling Pathway

ABSTRACT

Zika virus (ZIKV), a positive-sense single-stranded RNA virus, causes congenital ZIKV syndrome in children and Guillain-Barré Syndrome (GBS) in adults. ZIKV expresses nonstructural protein 5 (NS5), a large protein that is essential for viral replication. ZIKV NS5 confers the ability to evade interferon (IFN) signalling; however, the exact mechanism remains unclear. In this study, we employed affinity pull-down and liquid chromatography-tandem mass spectrometry (LC-MS/MS) analyses and found that splicing factor 3b subunit 3 (SF3B3) is associated with the NS5-Flag pull-down complex through interaction with NS5. Functional assays showed that SF3B3 overexpression inhibited ZIKV replication by promoting IFN-stimulated gene (ISG) expression whereas silencing of SF3B3 inhibited expression of ISGs to promote ZIKV replication. GTP cyclohydrolase I (GCH1) is the first and rate-limiting enzyme in tetrahydrobiopterin (BH4) biosynthesis. NS5 upregulates the expression of GCH1 during ZIKV infection. And GCH1 marginally promoted ZIKV replication via the IFN pathway. Additionally, GCH1 expression is related to the regulation of SF3B3. Overexpression of the SF3B3 protein effectively reduced GCH1 protein levels, whereas SF3B3 knockdown increased its levels. These findings indicated that ZIKV NS5 binding protein SF3B3 contributed to the host immune response against ZIKV replication by modulating the expression of GCH1.

1. Introduction

Zika virus (ZIKV) belongs to the mosquito-borne *Flavivirus* family of RNA viruses (Musso and Gubler, 2016; Barrows et al., 2018). It threatens global health, prompting the World Health Organization to declare it a public health emergency of international concern in 2016 (Musso et al., 2019; Wilder-Smith and Osman, 2020). Clinical manifestations of ZIKV infection in humans are characterized by a wide spectrum of symptoms that range from self-limited fever to serious neurological diseases such as Guillain–Barré Syndrome (GBS) (Barrows et al., 2018) and neonatal microcephaly (Leonhard et al., 2019). Unfortunately, currently no vaccines or antiviral drugs are available for ZIKV (Shan et al., 2018). Thus, a better understanding of the host-pathogen interaction of ZIKV is urgently needed to facilitate the development of novel therapeutic strategies.

ZIKV is a positive-sense single-stranded RNA virus with an envelope, and its genome that is approximately 11 kb long and consists of untranslated regions (UTRs) at both ends and an open reading frame (ORF) (Shi and Gao, 2017; Huber et al., 2019). The ORF encodes three structural proteins and seven nonstructural proteins (Guo et al., 2021). ZIKV NS5 is a nonstructural protein with the most conserved sequence and largest molecular weight. As a virus replication enzyme, it is not only responsible for genome replication and capping but also helps the virus escape from host immune responses (Zhao et al., 2021). In addition, NS5 has been used as an important target for antiviral drug design (Wang et al., 2018; Gharbi-Ayachi et al., 2020; Song et al., 2021). Since the epidemic, a series of breakthroughs have been achieved on the structure and function of ZIKV NS5 (Zhao et al., 2017). However, the mechanisms how the NS5 regulates host response is not entirely elucidated.

According to previous researches, ZIKV NS5 affects the production of new virions (Flory et al., 2021) and regulates the expression of various host factors (Limonta and Hobman, 2020). ZIKV NS5 interacts with host RIG-I, inhibits K63-linked polyubiquitination of RIG-I, suppresses the

* Corresponding authors.
E-mail addresses: lushuaiyao-km@163.com (S. Lu), pengxiaozhong@pumc.edu.cn (X. Peng).

https://doi.org/10.1016/j.virs.2022.12.005
Received 16 August 2022; Accepted 9 December 2022
Available online 23 December 2022

phosphorylation and nuclear localization of IRF3, and inhibits expression of interferon (IFN) β (Li et al., 2020). Furthermore, this inhibition depends on the MTase domain of NS5, and the D146 site of the NS5 conserved region was shown to be very important for suppression of the RIG-I signalling pathway (Li et al., 2020; Schilling et al., 2020). Roby showed that ZIKV NS5 inhibits JAK/STAT-dependent cytokine signalling in part by binding to cellular heat shock protein 90 (HSP90) (Roby et al., 2020). Notably, p53 has also recently been identified as an interacting partner of ZIKV NS5 in human neural progenitor cells, and ZIKV NS5 induces p53-mediated apoptosis (Li et al., 2021). *In vitro* experiments have shown that ZIKV NS5 interacts with endogenous Akt in Huh7.5 cells. Additionally, ZIKV NS5 is phosphorylated by Akt, and Akt inhibitors inhibit ZIKV replication; greater inhibition of ZIKV replication is achieved by specific Akt inhibitors than by nonspecific Akt inhibitors.

IFN responses are stimulated early during flavivirus infection (Diamond, 2009). Previous studies have reported that ZIKV has developed various strategies to antagonize type I IFN signaling (Lesage et al., 2022). NS5 has been reported to be involved in different stages of the IFN signalling cascade through diverse strategies (Best, 2017). ZIKV evades antiviral signaling, enhancing its replication through NS5-mediated proteasomal degradation of STAT2 (Best, 2017). ZIKV NS5 interacts with PAF1C to inhibit the expression of IFN-stimulating genes and ultimately abrogate the host antiviral response (Kovanich et al., 2019). However, the mechanism by which ZIKV NS5 inhibits IFN signaling requires further exploration.

Splicing factor 3b subunit 3 (SF3B3), an important gene that contributes to alternative spicing, is a member of the SF3B complex within the U2 snRNP (Stegeman et al., 2016). Recent studies show that SF3B3 plays a vital role in regulating the malignant phenotypes of various cancer types (Chen et al., 2017; Zhang et al., 2021). GTP cyclohydrolase I (GCH1) is a rate-limiting enzyme for tetrahydrobiopterin (BH4) synthesis (Wei et al., 2020). Additionally, the expression of GCH1 was higher in the chickens infected avian influenza viruses with shorter survival time (Uchida et al., 2012). However, little is known about the biological functions of SF3B3 and GCH1 in ZIKV infection.

Given the importance of NS5 in the ZIKV life cycle, we sought to comprehensively identify host factors associated with NS5 that modulate ZIKV replication using a mass spectrometry-based screening method. Here, we confirm the interaction of ZIKV NS5 with the host factor SF3B3 and report that ZIKV NS5 upregulates the expression of GCH1. Functional assays revealed the antiviral effect of SF3B3 and the proviral role of GCH1. Additionally, we identified GCH1 as a target gene of SF3B3. Decreased SF3B3 expression upregulated GCH1, thus stimulating ZIKV replication. Therefore, GCH1 may be a crucial host gene exploited by ZIKV to promote its replication, and targeting GCH1 may be a viable approach for better control of ZIKV infection.

2. Materials and methods

2.1. Cell lines and virus

U251 cells were purchased from the Cell Center of Peking Union Medical College (Beijing, China). U87MG and A549 cells were purchased from American Type Culture Collection (ATCC). Vero cells and HEK293T cells were obtained from the Institute of Medical Biology, Chinese Academy of Medical Sciences, and Peking Union Medical College (Kunming, China). U251 cells and U87MG cells were cultured in MEM supplemented with 10% foetal bovine serum (Gibco, Thermo Fisher Scientific, MA, USA), 1% nonessential amino acids (Gibco, Thermo Fisher Scientific, MA, USA), 2% sodium pyruvate (Gibco, Thermo Fisher Scientific, MA, USA), 100 U/mL ampicillin and 100 μg/mL streptomycin (Solarbio, Beijing, China). Vero cells and A549 cells were maintained in MEM supplemented with 10% foetal bovine serum, 100 U/mL ampicillin and 100 μg/mL streptomycin. HEK293T cells were cultured in DMEM with 10% foetal bovine serum, 100 U/mL ampicillin and 100 μg/mL streptomycin. All cells were cultured at 37 °C with 5% CO_2.

ZIKV was obtained using a reverse genetic system. The pACYC177-T7-ZIKV full-length clone (GenBank: KX253996.1) was previously constructed in our laboratory and linearized by *Nsi*I (NEB, MA, USA) digestion. The enzyme-digested product was used as a template for *in vitro* transcription with a mMESSAGE mMACHINE™ T7 kit (AM1344, Invitrogen); *in vitro*-transcribed RNAs were eluted in nuclease-free water. ZIKV was generated by transfecting of the *in vitro*-transcribed viral RNAs into Vero cells using Lipofectamine 3000 (L3000, Invitrogen, USA). The virus was amplified in Vero cells and stored at −80 °C. Virus titration was determined by performing a plaque assay using Vero cells.

2.2. Construction of plasmids and transfection

The Flag-tag was fused to the C-terminus of NS5 containing *Kpn*I and *Xho*I restriction sites through PCR amplification from the pACYC177-T7-ZIKV full-length clone to construct a plasmid encoding Flag-tagged ZIKV NS5. The Flag-tagged ZIKV NS5 fragment was digested and cloned into the *Kpn*I- and *Xho*I-cut pcDNA4.0 vector using T4 DNA ligase (NEB, MA, USA). Myc-tagged SF3B3 and GCH1 were amplified using HEK293T cells as the template and subsequently cloned into the pcDNA4.0 vector. The primers used are listed in Supplementary Table S1. Cells were seeded in 6-well plates or 10 cm culture dishes (Corning, USA), and then transfected with plasmids at 2.5 μg or 10 μg using Lipofectamine 3000 (L3000, Invitrogen, USA), respectively.

2.3. Antibodies

Primary antibodies against the following proteins or peptides were used: ZIKV NS5 (BF-6A1, BioFront, Tallahassee, Fla., USA), 1:1000 dilution for immunoblotting (IB) and 1:50 dilution for immunofluorescence (IF); ZIKV E (GTX133314, GeneTex, CA, USA), 1:1000 dilution for IB; ZIKV E (BF-1176-46, BioFront, Tallahassee, Fla., USA), 1:100 dilution for IF; Flag (#8146, CST, Danvers, MA, USA), 1:1000 dilution for IB; p-STAT3 S727 (ab32143, Abcam, Waltham, MA, USA), 1:1000 dilution for IB; STAT3 (10253-2-AP, Proteintech, China), 1:1000 dilution for IB; SF3B3 (14577-1-AP, Proteintech, China), 1:2000 dilution for IB and 1:100 dilution for IF; EIF4A3 (17504-1-AP, Proteintech, China), 1:2000 dilution for IB; RPS3A (ab171742, Abcam, Waltham, MA, USA), 1:10000 dilution for IB; and GCH1 (28501-1-AP, Proteintech, China), 1:2000 dilution for IB and 1:100 dilution for IF. An antibody against tubulin (TA503129, Origene, Maryland, USA) diluted 1:5000 for IB was employed as a loading control. The secondary antibodies used were as follows: iFluor™ 594-conjugated goat anti-rabbit IgG polyclonal antibody (HA1122, HUABIO, Hangzhou, China), 1:1000 dilution for IF; iFluor™ 488-conjugated goat anti-mouse IgG polyclonal antibody (HA1125, HUABIO, Hangzhou, China), 1:1000 dilution for IF; HRP-conjugated goat anti-mouse IgG (ZB-2305, ZSGB-BIO, Hangzhou, China), 1:10000 dilution for IB; and HRP-conjugated goat anti-rabbit IgG (ZB-2301, ZSGB-BIO, Hangzhou, China), 1:10000 dilution for IB.

2.4. Pull down and silver staining

Lysates of U251 cells expressing Flag and ZIKV NS5-Flag were prepared using IP lysis buffer (P0013, Beyotime, Shanghai, China) containing protease and phosphatase inhibitors (A32959, Thermo Scientific, MA, USA). The cell extracts were incubated with Anti-Flag Affinity Gel (P2282, Beyotime, Shanghai, China) for 12 h at 4 °C. After incubation, the affinity gel was washed with cold IP lysis buffer. The eluate was collected and visualized after separation on 10% SDS-PAGE gels followed by silver staining with a Fast Silver Stain Kit (P0017S, Beyotime, Shanghai, China). Proteins extracted from the gel were digested with trypsin and analysed using a liquid chromatography-tandem mass spectrometry (LC-MS/MS) system (Applied Protein Technology Co., Ltd., Shanghai, China).

2.5. Tandem mass tag (TMT)-based quantitative proteomic analysis

Three replicates of U251 cells transiently overexpressing ZIKV NS5 and corresponding control U251 cells per group were lysed with 40 μL of SDT buffer (100 mmol/L Tris, 1 mmol/L DTT, and 4% (w/v) SDS, pH = 7.6) supplemented with protease and phosphatase inhibitors (A32959, Thermo Scientific, MA, USA) for 30 min at 4 °C, followed by boiling for 10 min at 98 °C. Subsequently, the TMT-based quantitative proteomic analysis was performed at Shanghai Applied Protein Technology Co., Ltd.

2.6. Western blotting and coimmunoprecipitation

Total protein was extracted from whole cells using RIPA lysis buffer (89900, Thermo Scientific, MA, USA) containing protease and phosphatase inhibitors. Samples containing equal amounts of protein were separated on SDS-PAGE and transferred to PVDF membranes (#1620177, Bio-Rad). After blocking with 5% skim milk for 1 h at 25 °C, the membranes were incubated with primary antibodies at 25 °C for 2 h, followed by an HRP-linked secondary antibody at 25 °C for 1 h. The samples were detected using an enhanced chemiluminescence detection system (PK10001, Proteintech, China), and the intensity of protein expression was quantified using ImageJ software.

For immunoprecipitation (IP), U251 or U87MG Flag- and ZIKV NS5-Flag-overexpressing cells were lysed using ice-cold IP lysis buffer containing protease and phosphatase inhibitors. The supernatant was incubated with Anti-Flag Affinity Gel at 4 °C overnight with constant rotation. After the incubation, the affinity gel was washed five times with cold IP lysis buffer. The precipitated proteins were eluted by resuspending the affinity gel in 2× SDS-PAGE loading buffer and boiling it for 10 min at 98 °C. The boiled protein samples were subjected to SDS-PAGE followed by IB.

2.7. Immunofluorescence staining

U251 NC cells and ZIKV NS5-overexpressing cells and U251 mock- and ZIKV-infected cells were seeded in 24-well plates containing 20-mm glass coverslips. After 24 h, the culture medium was removed, and the cells were washed three times and fixed with 4% PFA in PBS at 25 °C for 15 min. The PFA-fixed cells were permeabilized with 1% Triton-100 for 10 min at 25 °C. The cells were blocked with PBS containing 3% FBS for 1 h at 25 °C and incubated with the primary antibodies: anti-ZIKV NS5, anti-ZIKV E, anti-SF3B3, anti-GCH1 at 4 °C overnight. After three washes with PBS-T, incubation with the secondary antibodies: iFluor™ 594-conjugated goat anti-rabbit IgG polyclonal antibody, iFluor™ 488-conjugated goat anti-mouse IgG polyclonal antibody was performed for 1 h, followed by 3 washes with PBS. Images were captured using a Leica TCS SP8 microscope (Germany).

2.8. Nuclear and cytoplasmic fractionation

A Nuclear and Cytoplasmic Protein Extraction Kit (P0028, Beyotime, Shanghai, China) was used to separate the nuclear and cytoplasmic protein components according to the manufacturer's instructions. Briefly, cells were resuspended in 200 μL cytoplasmic protein extraction buffer A with PMSF and incubated on ice for 15 min. Then, 10 μL cytoplasmic protein extraction buffer B was added. Cells were incubated on ice for 1 min and centrifuged at 12, 000×*g* for 5 min at 4 °C. Supernatant (cytoplasm) was separated from pellet. Cell pellets were resuspended in 50 μL nucleoplasm protein extraction buffer with PMSF and vortexed 15 s every 2 min for 30 min. The suspension was centrifuged at 12, 000×*g* for 10 min at 4 °C. Supernatant (nucleoplasm) was separated from pellet.

2.9. siRNA-mediated transient knockdown

Cells were transfected with 50 nmol/L (final concentration) siRNAs using GP-transfect-Mate (Gene Pharma Co., Ltd., China), and were used for the following experiments 48 h after transfection. siRNAs against human SF3B3 (siSF3B3) and GCH1 (siGCH1) and the negative control siRNA (siNC) were produced by Gene Pharma (Gene Pharma Co., Ltd., China). The sense and antisense sequences of siRNAs are listed in Supplementary Table S2.

2.10. Plaque-forming assay

Tenfold dilutions of virus samples were added to monolayers of confluent Vero cells in 6-well plates at 37 °C for 1 h. After the incubation, the inocula were removed, and the cells were overlaid with 2 mL of MEM containing 1% low-melting-point agarose, 2% FBS, 100 U/mL ampicillin and 100 μg/mL streptomycin. After three days, the monolayers were stained with 0.1% neutral red, and plaques were counted.

2.11. qRT-PCR

Briefly, total RNA was extracted with TRIzol (Qiagen, Germany). RNA quality and quantity were assessed using a NanoDrop2000 spectrophotometer (Thermo Fisher Scientific, Waltham, MA, USA). Equal amounts of total RNA were subjected to reverse transcription for cDNA synthesis using a PrimeScript™ RT reagent Kit with gDNA Eraser (RR047A, Takara, Otsu, Japan). qRT-PCR was conducted by using cDNAs and SsoFast EvaGreen Supermix (1725202, Bio-Rad, Foster City, CA, USA) according to the manufacturer's instructions and a Bio-Rad CFX96 System (Bio-Rad, Foster City, CA, USA). qPCRs were performed in triplicate. β-Actin was used as a reference gene for mRNAs. The primer sequences used for qRT-PCR are listed in Supplementary Table S1.

2.12. Luciferase reporter assay

HEK293T cells cultured in 24-well plates were transfected with 100 ng of the ISRE-luc reporter plasmid, 5 ng of the pRL-TK reporter plasmid and 400 ng of a plasmid expressing the indicated proteins or empty plasmid. Similarly, HEK293T cells were transiently co-transfected with 100 ng of the ISRE-luc reporter plasmid, 5 ng of the pRL-TK reporter plasmid and 50 nmol/L (final concentration) siRNAs. At 24 h after transfection, the cells were stimulated with 1 ng/mL IFNβ or IFNγ (Peprotech, USA) for an additional 12 h. Cell lysates were used to determine luciferase activity using a Dual Luciferase Reporter Assay System (E1910, Promega, USA) according to the manufacturer's protocol; firefly luciferase activity levels were normalized to those of Renilla luciferase.

2.13. Cycloheximide chase assay

GCH1-overexpressing U87MG cells transfected with 50 nmol/L (final concentration) SF3B3 siRNA or siNC and 48 h post transfection were treated with 50 mg/mL Cycloheximide (CHX) (C7698, Sigma-Aldrich, St. Louis, Missouri, USA). Protein lysates were collected following 0, 6 or 12 h exposure to CHX. Western blotting was performed as described above.

2.14. Statistical analysis

Statistical significance was examined using GraphPad Prism software version 8.0. All data are presented as the means ± SEM, and each experiment was performed with three biological replicates. Comparisons between two groups were performed using Student's *t*-test (two-tailed), while multiple comparisons were performed using one-way analysis of (ANOVA). Differences were considered to be statistically significant at $P < 0.05$. $^{*}P < 0.05$, $^{**}P < 0.01$, and $^{***}P < 0.001$.

3. Results

3.1. SF3B3 interacts with ZIKV NS5

We first sought to identify potential host factors interacting with ZIKV NS5 that regulate virus infection or innate immunity. NS5 with a C-terminal Flag tag was expressed in U251 cells and conjugated to Anti-Flag affinity gel along with Flag as a negative control to capture interacting proteins that bind to NS5. In contrast to the negative control group, the ZIKV NS5-Flag-overexpressing group showed enrichment of some differentially altered bands. Subsequently, we excised and trypsinized whole protein bands and analysed them using LC-MS/MS (Fig. 1A and B). We identified 52 cellular candidate proteins interacting with ZIKV NS5 compared to negative control group (Supplementary Table S3). The data from the GO analysis showed that 15 of these proteins were most enriched in terms related to splicing-related factors (Fig. 1C and D). After ranking the proteins using propensity score matching (PSM), we selected several of the top splicing-related factors for a follow-up analysis (Supplementary Table S3). Subsequently, Flag-tagged ZIKV NS5 was individually expressed in U251 and U87MG cells, and extracts were used for co-IP assays and Western blot analysis; as a control, the same procedure was performed with an empty vector. Co-precipitation of SF3B3, EIF4A3, and RPS3A was observed with NS5 (Fig. 1E and F). Together, these data indicate that SF3B3 interacts with ZIKV NS5 in transiently transfected glioma cells.

3.2. SF3B3 is a host factor restricting ZIKV infection via IFN signalling pathway

In ZIKV infected U251 and U87MG cells, it showed that the SF3B3 protein level was downregulated following virus infection (Fig. 2A and

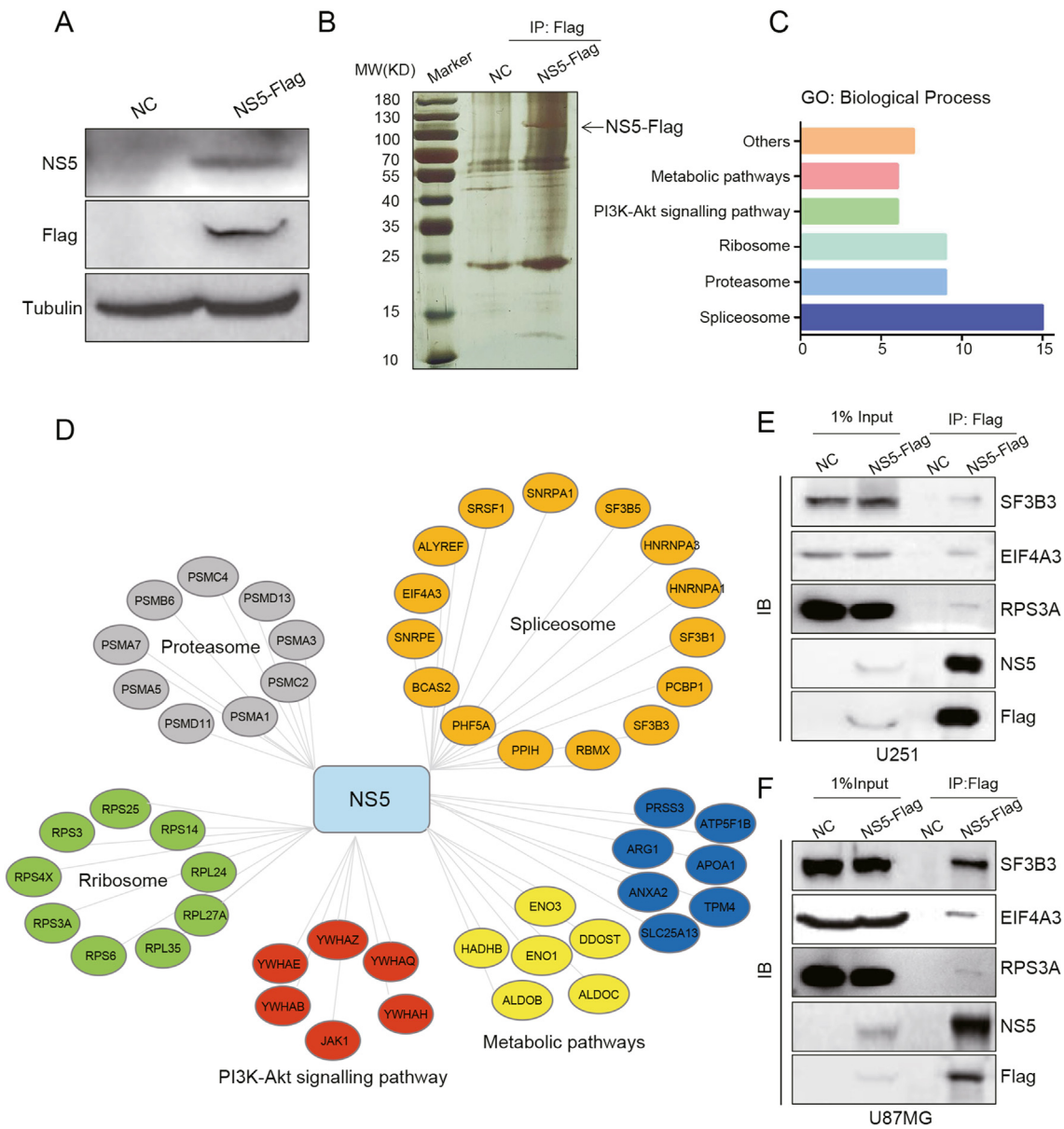

Fig. 1. SF3B3 is a host factor interacting with NS5. **A** Western blot showing the expression of NS5 in U251 cells transfected with the empty vector (NC) or ZIKV NS5 overexpression vector. **B** Identification of the NS5 complex pulled down by Anti-Flag Affinity Gel using protein extracts from U251 cells transfected with the empty vector (NC) or ZIKV NS5 overexpression vector. **C** The major functional categories of host proteins interacted with ZIKV NS5 are depicted. Mass spectrometry analysis of host proteins from NS5 complex of the affinity gel. **D** Interactions of ZIKV NS5 and host proteins identified by mass spectrometry. (**E**, **F**) SF3B3 interacts with ZIKV NS5 both in U251 and U87MG cells. Whole-cell extracts from U251 and U87MG cells expressing NC or NS5-Flag were subjected to immunoprecipitation with Anti-Flag Affinity Gel followed by immunoblotting (IB) with specific antibodies against the indicated proteins. All experiments were independently repeated three times.

B). To assess the role of SF3B3 in ZIKV infection, cells were transfected with a specific SF3B3-targeted siRNA (siSF3B3). Treatment with siSF3B3 following ZIKV infection successfully reduced SF3B3 protein expression in U251 and U87MG cells (Fig. 2C). Compared with the negative control group, the abundance of ZIKV E protein was markedly increased in U251 and U87MG cells with SF3B3 silencing (Fig. 2C). We then analysed the effect of SF3B3 knockdown on plaque formation. Vero cells were incubated with cell supernatants from Fig. 2C. Compared with the negative control group, the plaque-forming units were markedly increased in the SF3B3 silencing group (Fig. 2D). These data show that silencing SF3B3 promotes ZIKV replication. Then we assessed whether SF3B3 overexpression inhibits ZIKV replication. It was confirmed that SF3B3 overexpressing significantly reduced ZIKV proliferation and plaque formation in U251 and U87MG cells infected with ZIKV (Fig. 2E and F). In summary, these results show that SF3B3 negatively modulates ZIKV proliferation.

We described the antiviral function of SF3B3, but the ability of SF3B3 to regulate IFN signaling remains largely unknown and has not been reported previously, which inspired us to investigate the role of SF3B3 in regulating the antiviral immune response. IFN response in restricting flavivirus infection has been confirmed (Diamond, 2009). STAT3 activated in response to IFN stimulation located in the ISRE inducing ISG expression against virus infection (Mahony et al., 2017). Here, we transfected HEK293T cells with an ISRE promoter-driven luciferase reporter, internal control Renilla luciferase reporter and vector encoding SF3B3 or the empty vector. SF3B3 substantially increased ISRE promoter-driven luciferase activity after IFNβ or IFNγ stimulation, while ISRE promoter-driven luciferase activity was decreased when SF3B3 was

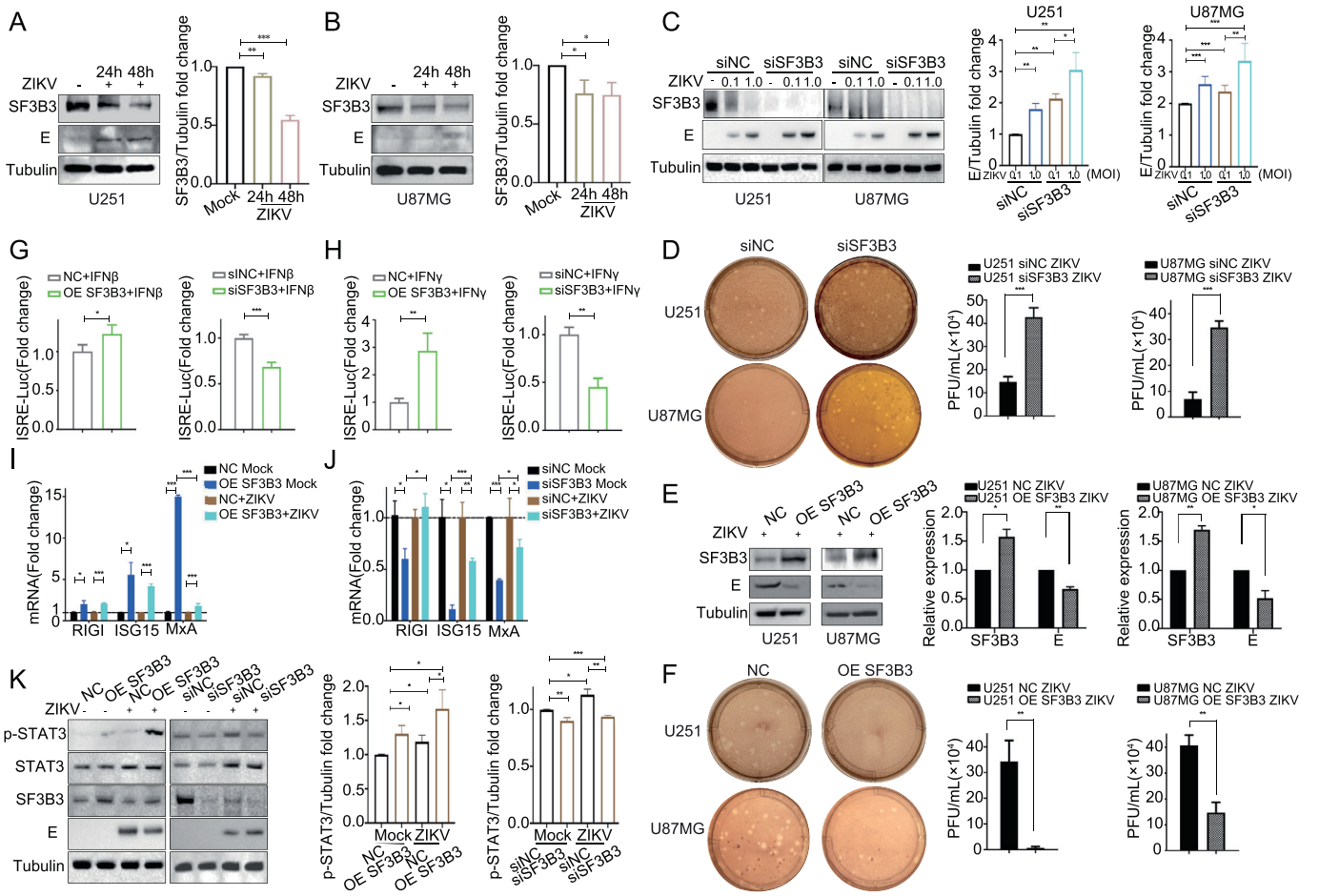

Fig. 2. Silencing SF3B3 enhances ZIKV replication via IFN signalling. (**A**, **B**) Levels of the SF3B3 protein in U251 and U87MG cells subjected to mock or ZIKV infection (MOI: 0.1) for 24 h and 48 h were measured using Western blotting. **C** ZIKV E protein was increasingly expressed following SF3B3 silencing in ZIKV infected U251 and U87MG cells. U251 and U87MG cells were transfected with a nonrelated siRNA (siNC) or specific siRNA against SF3B3 for 48 h followed by infection with ZIKV (MOI = 0, 0.1, and 1) for 48 h. **D** SF3B3 knockdown promotes plaque formation. Vero cells were treated with the cellular supernatants of ZIKV infection (MOI = 0.1) group collected in (**C**) for 1 h at 37 °C. The plaque assay was performed to compare the cytopathic effect. **E** The expression of ZIKV E protein was downregulated following SF3B3 overexpression in ZIKV infected U251 and U87MG cells. U251 and U87MG cells were transfected with the empty vector (NC) or SF3B3-Myc overexpression vector and then infected with ZIKV (MOI: 0.1) for 48 h. Cellular supernatants were collected. The expression levels of SF3B3 and ZIKV E protein were measured using Western blotting. **F** SF3B3 inhibits plaque formation. Vero cells were treated with the cellular supernatants of ZIKV infection (MOI: 0.1) group collected in (**E**) for 1 h at 37 °C. The plaque assay was performed to compare the cytopathic effect. (**G**, **H**) Effects of SF3B3 on IFNβ/IFNγ-induced ISRE promoter activation. HEK293T cells were transfected with the indicated protein expression plasmid or siRNA, the ISRE reporter plasmid and the pRL-TK reporter plasmid for 24 h. The cells were then treated with IFNβ or IFNγ as described in the Materials and Methods. Twelve hours later, cell lysates were assayed for luciferase activity. (**I**, **J**) SF3B3 induced antiviral genes expression. **I** A549 cells were transfected with NC or the SF3B3 overexpression plasmids following mock or ZIKV infection. **J** A549 cells were transfected with siNC or SF3B3 siRNA following mock or ZIKV infection. Cells were harvested at 24 hpi, and the expression levels of RIG-I, ISG-15, and MxA were examined using qRT-PCR. **K** SF3B3 increased phosphorylation of STAT3 on S727. U251 cells were transfected with NC or the SF3B3-overexpression plasmid, or siNC or siSF3B3 RNA following ZIKV (MOI = 0 and 0.1) infection, respectively. After 48 h, total cellular proteins were collected and subjected to Western blotting using antibodies against STAT3, p-STAT3, ZIKV E, SF3B3 and tubulin. All experiments were independently repeated three times. Data are presented as the means ± SEM. Comparisons between two groups were performed using unpaired two-tailed Student's *t*-test, while multiple comparisons were performed using one-way analysis of variance (ANOVA) with Dunnett's test. $^{*}P < 0.05$, $^{**}P < 0.01$, and $^{***}P < 0.001$.

knocked down (Fig. 2G and H). Subsequently, we examined the endogenous induction of RIG-I and ISG expression after mock and ZIKV infection in A549 cells. The expression of the pattern recognition receptor RIG-I, which detects viral RNA, was increased in SF3B3-overexpressing cells but decreased in SF3B3-knockdown cells. Similar to ISRE promoter-driven luciferase reporter activation, SF3B3 substantially promoted the production of ISGs, including ISG15 and MxA (Fig. 2I and J). Additionally, the stimulation of SF3B3 to ISG genes, particularly MxA, was attenuated to some extent by ZIKV infection (Fig. 2I and J), verifying the antagonistic effect of ZIKV on the antiviral response of host cells. As STAT signalling acts upstream of ISG production, the extent of STAT phosphorylation was also analysed in SF3B3-overexpressing and SF3B3-knockdown U87MG cells during ZIKV infection. Western blotting confirmed that ZIKV infection promoted STAT3 phosphorylation (Fig. 2K). Moreover, SF3B3 overexpression promoted STAT3 phosphorylation but SF3B3 silencing significantly inhibited phosphorylation under ZIKV infection and mock infection (Fig. 2K). In contrast, ZIKV NS5 inhibited ISRE promoter-driven luciferase activity after IFNβ or IFNγ stimulation (Supplementary Fig. S1) and reduced the levels of STAT3 and p-STAT3 (Supplementary Fig. S2). Collectively, these results indicate that SF3B3 functions as a host factor restricting ZIKV replication via the IFN signalling pathway.

3.3. NS5-mediated upregulation of GCH1 correlates positively with ZIKV infection

Proteomic profiling of three NS5-overexpressing samples and three negative control samples with empty vector was performed using TMT-based quantitative proteomic technology to further explore the target genes of the NS5-interacting protein SF3B3. Differentially expressed proteins were identified according to the criteria of a minimum 1.2-fold change in expression (greater than 1.2-fold upregulation; less than 0.83-fold downregulation) and a P value < 0.05. Eighteen proteins were identified. Twelve of these proteins were identified to be upregulated and

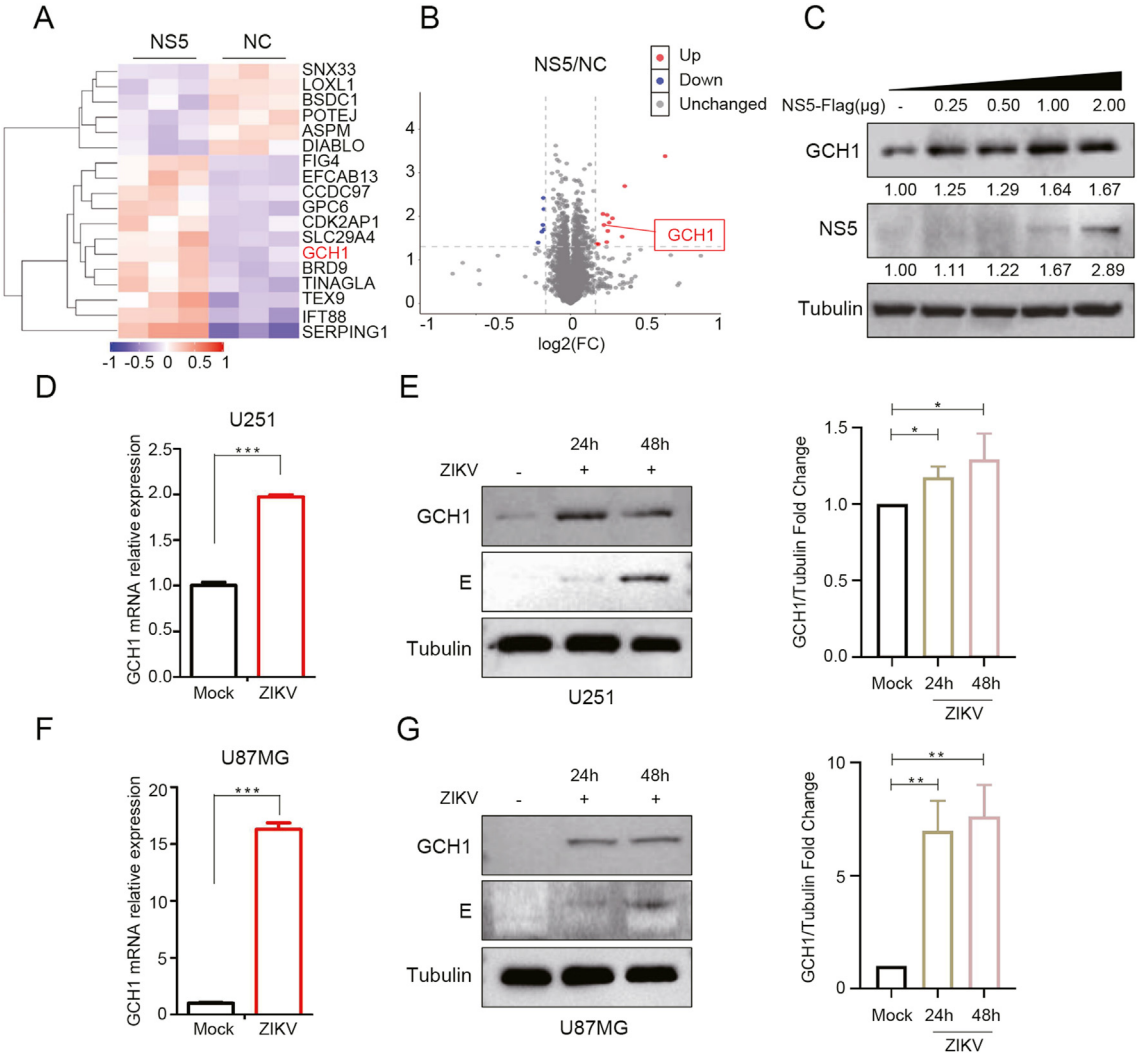

Fig. 3. GCH1 protein is actively induced by ZIKV infection and is positively correlated with NS5. (**A, B**) Identification of host genes regulated by ZIKV NS5 using a proteomics analysis. **A** Heatmap showing the unsupervised clustering of differentially expressed genes regulated by ZIKV NS5 in U251 cells. **B** Volcano plot showing the variation in gene expression of U251 cells after NS5 transfection. Upregulated genes (red) and downregulated genes (blue) with a fold change>1.2 and $P < 0.05$ are shown. **C** NS5 induced the expression of GCH1 in a dose-dependent manner. U251 cells were transfected with increasing amounts of ZIKV NS5-Flag for 48 h, and the protein expression levels of NS5 and GCH1 were analysed using Western blotting. (**D–G**) GCH1 expression was induced after ZIKV infection. (**D, F**) RT-qPCR analysis of GCH1 mRNA levels in mock- and ZIKV infected (MOI = 0.1) U251 and U87MG cell lines at 24 h postinfection at an. β-Actin was used as an internal reference. (**E, G**) U251 and U87MG cells were infected without or with ZIKV at an MOI of 0.1 for 48 h, and the cells were harvested for immunoblotting. All experiments were independently repeated three times. Data are presented as the means ± SEM. Comparisons between two groups were performed using unpaired two-tailed Student's *t*-test, while multiple comparisons were performed using one-way analysis of variance (ANOVA) with Dunnett's test. *$P < 0.05$, **$P < 0.01$, and ***$P < 0.001$.

eight to be downregulated upon NS5 overexpression compared with the negative control group (Fig. 3A and B). Among these genes, GCH1 is closely related to the host antiviral immune response, according to previous studies. For example, the GCH1 protein correlates with survival in chickens infected with recombinant viruses of a highly pathogenic avian influenza virus (Uchida et al., 2012). Additionally, high expression of GCH1 influences the evolution of antimalarial antifolate drug resistance, whereas GCH1 mutation is associated with inflammatory pain disorders (Khairallah et al., 2021). We first transfected cells with an NS5 overexpression plasmid to determine whether the dynamics of GCH1 expression are affected by NS5. Western blotting assay showed that the GCH1 level gradually increased as the expression of ZIKV NS5 increased (Fig. 3C). Additionally, GCH1 mRNA expression was upregulated in ZIKV-infected U251 and U87MG cell lines (Fig. 3D and F). Consistently, the GCH1 protein level was increased following ZIKV infection (Fig. 3E and G). These results demonstrated that GCH1 upregulation induced by ZIKV infection is positively correlated with NS5 protein.

3.4. GCH1 promotes ZIKV replication by inhibiting the IFN signalling pathway

To date, no reports have described whether ZIKV modulates host GCH1 expression to facilitate its replication. Hence, we sought to explore the regulatory effect of GCH1 on ZIKV replication by transfecting U251 and U87MG cells with GCH1-targeted siRNA (siGCH1) following ZIKV infection. siGCH1 treatment resulted in a reduction of the GCH1 and

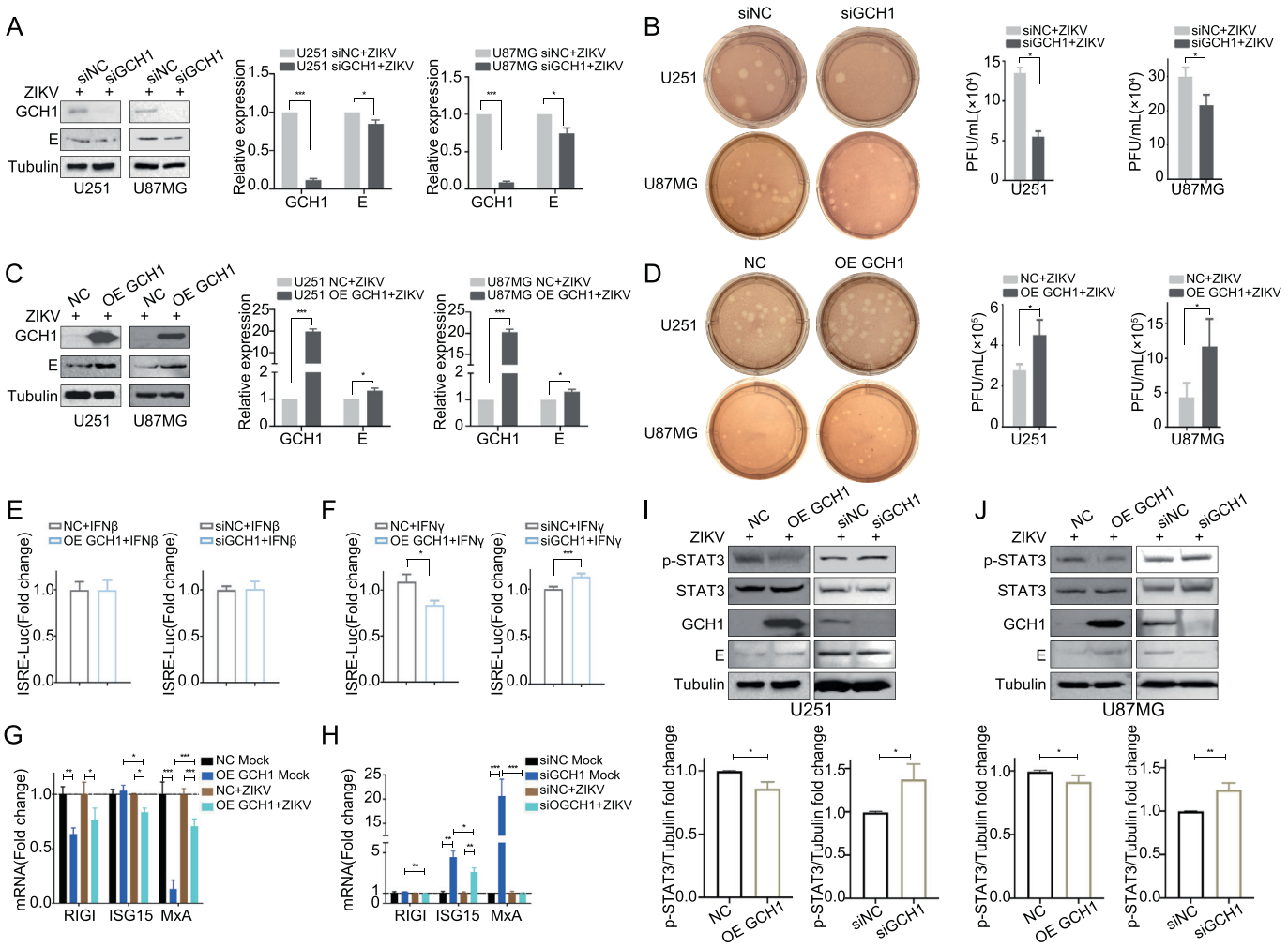

Fig. 4. GCH1 promotes ZIKV replication by inhibiting the IFN signalling pathway. **A** U251 and U87MG cells were transfected with a nonrelated siRNA (siNC) or specific siRNAs targeting GCH1 for 48 h, followed by infection with ZIKV (MOI: 0.1) for 48 h. **B** Vero cells were treated with the cellular supernatants collected in (**A**) for 1 h at 37 °C. The plaque assay was performed to compare the cytopathic effect in siNC and siGCH1 groups. (**C**, **D**) GCH1 promotes ZIKV replication. **C** U251 cells were transfected with the empty vector (NC) or GCH1-Myc overexpression vector and then exposed to ZIKV infection (MOI: 0.1) for 48 h. Cellular supernatants were collected and the expression levels of GCH1 and ZIKV E were measured using Western blotting. **D** Vero cells were treated with the cellular supernatants collected in (**C**) for 1 h at 37 °C. The plaque assay was performed to compare the cytopathic effect in NC and GCH1 overexpression group. (**E**, **F**) Effects of GCH1 on IFNβ/IFNγ-induced ISRE promoter activation. HEK293T cells were transfected with the indicated protein expression plasmid or siRNA, the ISRE reporter plasmid and the pRL-TK reporter plasmid. The cells were treated with IFNβ or IFNγ, as described in the Materials and Methods. Twelve hours later, cell lysates were assayed for luciferase activity. (**G**, **H**) GCH1 inhibited antiviral genes expression. **G** A549 cells were transfected with NC and GCH1 overexpression plasmids following ZIKV infection. **H** A549 cells were transfected with siNC or specific siRNAs against GCH1 following ZIKV infection. Cells were harvested 24 hpi, and the expression levels of RIG-I, ISG-15, and MxA were examined using qRT-PCR. (**I**, **J**) GCH1 decreased phosphorylation of STAT3 on S727. U251 and U87MG cells were transfected with NC or GCH1 overexpression plasmid or siNC and siSF3B3 RNA following ZIKV infection. After 48 h, total cellular proteins were collected and subjected to Western blotting using antibodies against STAT3, p-STAT3, ZIKV E, GCH1 and tubulin. All experiments were independently repeated three times. Data are presented as the means ± SEM. Comparisons between two groups were performed using unpaired two-tailed Student's *t*-test, while multiple comparisons were performed using one-way analysis of variance (ANOVA) with Dunnett's test. $^{*}P < 0.05$, $^{**}P < 0.01$, and $^{***}P < 0.001$.

ZIKV E protein levels in U251 and U87MG cells, respectively (Fig. 4A). The plaque-forming assay showed reduced plaques in siGCH1 treated cells compared with the negative control siRNA (siNC) treatment group (Fig. 4B). Additionally, we further validated the proviral effect of GCH1 by an GCH1 overexpression plasmid. First, the transfection efficiency was confirmed by detecting the high expression level of GCH1 protein in U251 and U87MG cells infected with ZIKV (Fig. 4C). As shown in Fig. 4C and D, ZIKV E protein level and the number of viral plaques were significantly increased by forced expression of GCH1 in U251 and U87MG cells. In summary, all these findings strongly support a role for GCH1 as a host proviral factor in ZIKV propagation.

Further, we examined the regulatory effect of GCH1 on the IFN signalling pathway and found that its overexpression inhibited IFNγ-mediated but not IFNβ-mediated ISRE activity (Fig. 4E and F). Overexpression of GCH1 reduced the levels of the RIG-I, ISG-15, and MxA mRNA upon ZIKV infection (Fig. 4G), and the expression level of ISG15 was significantly increased when GCH1 was silenced during ZIKV infection (Fig. 4H). Additionally, Western blotting confirmed that GCH1 overexpression inhibited STAT3 phosphorylation (Fig. 4I and J); in contrast, GCH1 silencing promoted STAT3 phosphorylation (Fig. 4I and J). Together, it suggests that GCH1 regulates the IFN signalling pathway through the phosphorylation of STAT3.

3.5. ZIKV infection induces the expression of GCH1 through a mechanism regulated by SF3B3

We have clarified that the NS5-binding protein SF3B3 exerts a stimulatory effect on the IFN pathway. Moreover, the NS5-mediated upregulation of the GCH1 protein is reported to induce immunosuppression (Wei et al., 2021). We next investigated whether GCH1 is a downstream target of SF3B3. The expression of GCH1 was evaluated in SF3B3-overexpressing and -knockdown cells following ZIKV infection. Compared with the control group, the expression levels of the GCH1 protein were significantly decreased in the SF3B3-overexpressing group. Consistently, transfection of siSF3B3 significantly increased GCH1 protein expression levels (Fig. 5A and B). In addition, a CHX pulse-chase assay was performed to examine the effect of SF3B3 on GCH1 stability. As shown in Fig. 5C, SF3B3 knockdown slowed the degradation of GCH1. Taken together, SF3B3 promotes the degradation of GCH1. As GCH1 expression is regulated by SF3B3 in ZIKV-infected glioma cells, we knocked down SF3B3 in GCH1-silenced U87MG cells following ZIKV infection and analysed the effects on ZIKV proliferation. We found that SF3B3 knockdown significantly rescued ZIKV E protein expression and viral plaque formation in GCH1-silenced U251 cells (Fig. 5D). Collectively, these results indicate that SF3B3 inhibits ZIKV replication by targeting GCH1.

3.6. Subcellular localization of SF3B3 and GCH1

It has been reported some viral proteins can alter the localization of certain host factors by regulating their nuclear-cytoplasmic shuttling (Sajidah et al., 2021). In this study, we examined the subcellular localization of SF3B3 and GCH1 after NS5 overexpression and ZIKV infection by immunostaining and confocal microscopy analysis. Overall, the expression of ZIKV NS5 and ZIKV infection didn't change the subcellular localization of SF3B3 and GCH1 (Fig. 6A–D). Similar results were obtained from the nuclear and cytoplasmic fractionation by Western blotting assays (Fig. 6E). Taken together, ZIKV infection does not alter the subcellular localization of SF3B3 and GCH1.

4. Discussion

An understanding of the regulatory mechanisms in ZIKV-infected cells will allow us to obtain insights into the disease pathogenesis and treatment of patients. The antiviral immune response is a complicated process (Ngono and Shresta, 2018). Type I IFN and the downstream STAT signalling pathway, which are vital components of the innate immune system, play crucial roles in mammalian host defences against viral

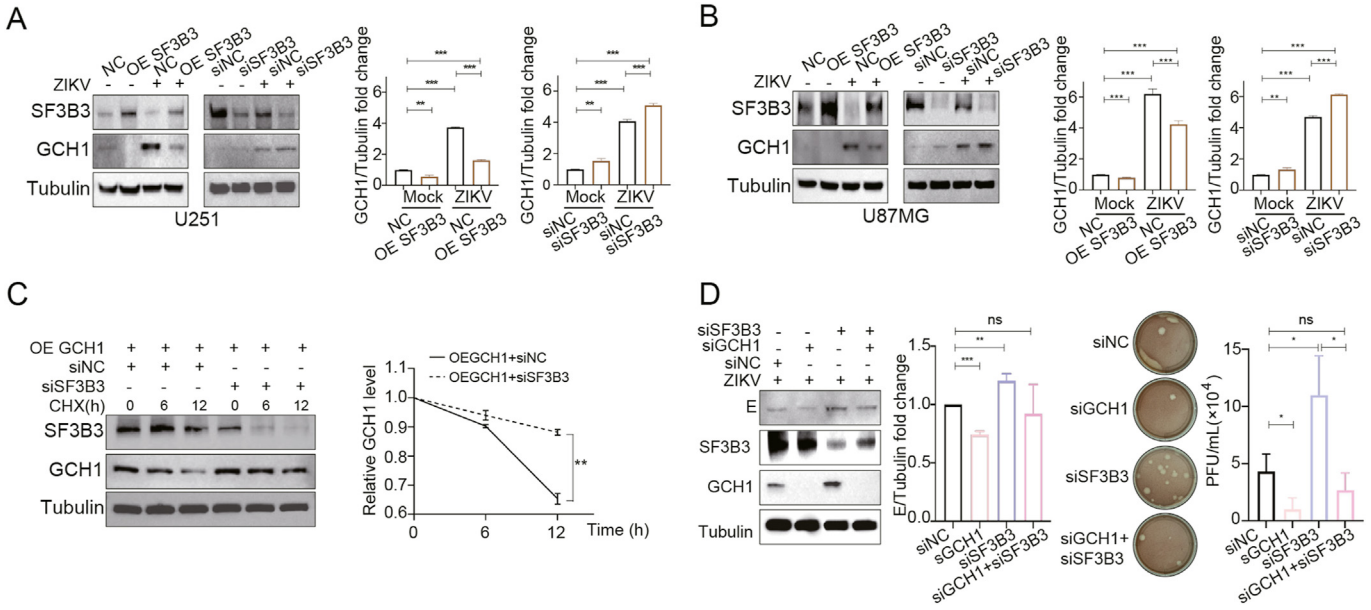

Fig. 5. ZIKV infection induces the expression of GCH1 which was negatively regulated by SF3B3. (**A**, **B**) SF3B3 negatively correlates with GCH1 expression level in ZIKV-infected U251 and U87MG cells. **A** U251 cells were transfected with NC, or SF3B3 overexpression vector. After transfection 24 h, cells were ZIKV infected (MOI = 0.1) or mock infected for 48 h. **B** U87MG cells were transfected with siNC, or siSF3B3 RNA. After transfection 24 h, cells were ZIKV infected (MOI = 0.1) or mock infected for 48 h. **C** SF3B3 promotes degradation of GCH1. GCH1-overexpressed U87MG cells were incubated with 50 nmol/L SF3B3 siRNA or siNC for 48 h and then treated with 50 mg/mL CHX. GCH1 expression was analysed using immunoblotting. **D** GCH1 knockdown reverses the promoting effects of siSF3B3 on ZIKV replication. SF3B3 was knocked down in U251 GCH1-knockdown or control cells. The plaque formation assay was performed, and plaque-forming units were counted. All experiments were independently repeated three times. Data are presented as the means ± SEM. Comparisons between two groups were performed using unpaired two-tailed Student's *t*-test, while multiple comparisons were performed using one-way analysis of variance (ANOVA) with Dunnett's test. $^{*}P < 0.05$, $^{**}P < 0.01$, and $^{***}P < 0.001$.

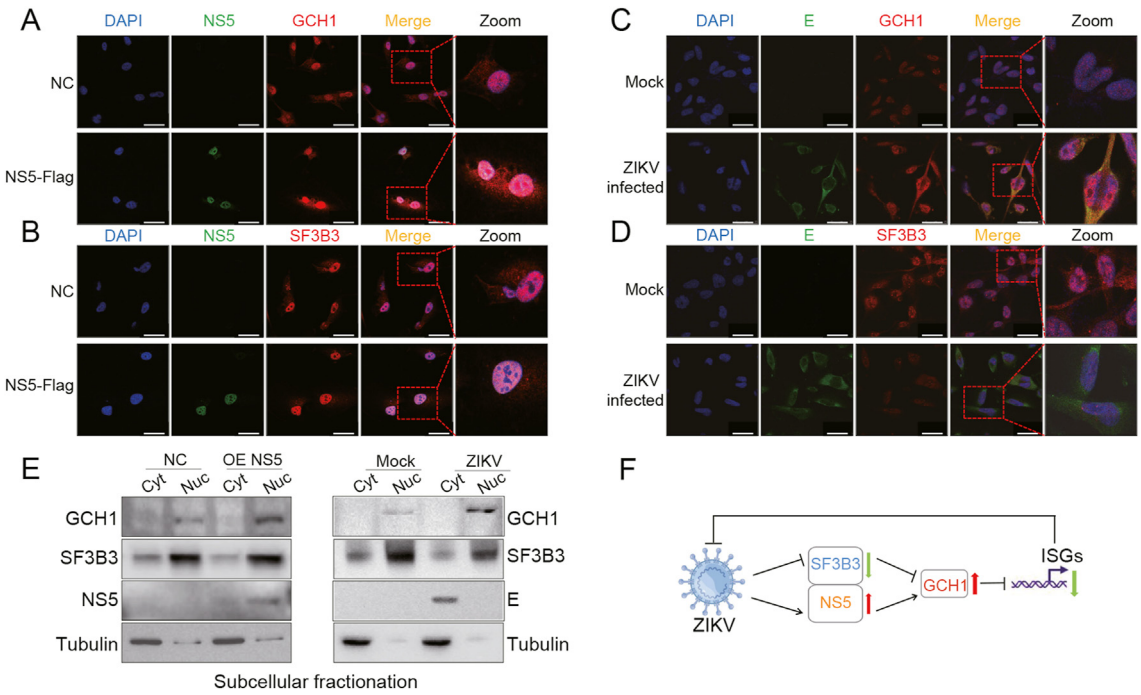

Fig. 6. Subcellular localization of SF3B3 and GCH1 and graphical illustration of the interaction between them. (**A**–**D**) Immunofluorescence colocalization was imaged using a confocal microscope. Scale bar, 25 μm. (**A**–**B**) Subcellular localization of SF3B3, GCH1 and ZIKV NS5 in NC- and NS5-Flag-transfected U251 cells. (**C**–**D**) Subcellular localization of SF3B3, GCH1, and ZIKV E in mock- and ZIKV-infected U251 cells. (**E**) The protein levels of SF3B3, GCH1 and ZIKV NS5 in subcellular fractions from NC or NS5-Flag U251 cells, and the levels of SF3B3, GCH1 and ZIKV E in subcellular fractions from mock- or ZIKV-infected U251 cells were detected using Western blotting (Nuc: nucleoplasm, Cyt: cytoplasm). All experiments were independently repeated three times. (**F**) Schematic representation of the mechanism by which the NS5-binding protein SF3B3 and GCH1 regulate ZIKV replication. The schematic diagram was generated with www.figdraw.com.

infection (Chen et al., 2018). Previous studies have reported that ZIKV antagonizes type I IFN signalling through various molecular defence strategies to maintain infection (Ren et al., 2021). Certain viral proteins, such as NS2A (Fanunza et al., 2021), NS4B (Fanunza et al., 2021), and NS5 (Zhao et al., 2021), antagonize the IFN response following ZIKV infection over time. Although ZIKV NS5, one of the most potent type I IFN antagonists (Best, 2017), has been documented to play an important role in promoting ZIKV infection (Thurmond et al., 2018), the mechanism by which NS5 senses ZIKV invasion remains unclear.

ZIKV utilizes host factors throughout its life cycle (Shah et al., 2018; Guo et al., 2021). Thus, more host factors regulated by ZIKV NS5 must be characterized to understand their roles during viral infection. Using immunoprecipitation of EGFP-tagged proteins to capture the NS5 interactome, Duangnapa Kovanich et al. reported that 30 proteins (including SF3B3, SF3B1, and RBMX) may be shared NS5-interacting proteins among JEV and ZIKV (Kovanich et al., 2019). Another study reported that SF3B3 might play a crucial role in the progression of hand, foot, and mouth disease (HFMD) (Lin et al., 2020). Schreiber et al. used a high-throughput siRNA screening method to show that multiple U2 snRNP spliceosome family members, including SF3B3, induce host-mediated restriction of recombinant adeno-associated viruses (Schreiber et al., 2015). Furthermore, Meng Miao et al. used proteomic strategies to show that SF3B3 is downregulated in K562 cells infected with dengue virus (Miao et al., 2019). To date, however, little is known about the role of SF3B3 in ZIKV infection. In the present study, we identified SF3B3, a member of the U2 snRNP spliceosome, interacted with ZIKV NS5 (Finci et al., 2018). Our study provides evidence that SF3B3 downregulation in ZIKV-infected glioma cells confers antiviral activity (Fig. 6F). The expression levels of RIG-I, ISG-15, and MxA were increased in parallel with SF3B3 upregulation.

Many studies have reported that ZIKV is highly dependent on the abnormal expression of host factors for its replication. Krystal A Fontaine et al. reported that ZIKV capsid targets UPF1 for degradation, resulting in enhanced ZIKV infection (Fontaine et al., 2018). In this study, we identified that NS5 is able to induce the expression of GCH1. Overexpression of GCH1 resulted in decreased expression levels of components of the IFN signalling cascade, such as ISG-15 and MxA, contributing to its proviral activities. Additionally, the expression of the GCH1 protein was negatively regulated by SF3B3. Moreover, a knockdown-rescue experiment showed that SF3B3 silencing rescued ZIKV replication in GCH1-depleted cells. Therefore, our study reveals an important SF3B3-GCH1 signalling axis involved in ZIKV infection (Fig. 6F). GCH1 might be an efficient target for ZIKV infection therapeutic treatment. Specific small molecular inhibitors targeting GCH1 might be next research direction.

Members of the STAT family are critical transcription factors required for the activation of IFN-stimulated antiviral genes (Ivashkiv and Donlin, 2014; Nan et al., 2017). In addition, phosphorylation of the STAT family leads to enhanced transcriptional activity. ZIKV NS5 might interfere with the type I IFN response by blocking the phosphorylation of STAT1 (Hertzog et al., 2018), while MxA inhibits ZIKV propagation by promoting the phosphorylation of STAT1 and STAT2 (Ren et al., 2021). The conclusion can be further confirmed by our results showing that the expression of STAT3 and p-STAT3 was downregulated in ZIKV NS5 overexpression U87MG cells. While, antiviral response can be induced under ZIKV infection. Our finding is consistent with a recent report demonstrated that phosphorylation of STAT3 was up-regulated in ZIKV infection cells, which supports the idea that STAT3 activation is important in ZIKV infection (Zhu et al., 2017). We have previously confirmed that both SF3B3 and GCH1 regulate ISG expression, although their ability to modulate upstream STAT signalling is a question that needs to be addressed. Our results show that SF3B3 overexpression results in increased phosphorylation of STAT3, and GCH1 overexpression leads to decreased phosphorylation of STAT3. Therefore, we speculate that phosphorylation of STAT3 could be inhibited through SF3B3 downregulation and GCH1 upregulation by ZIKV infection, resulting in promotion of virus proliferation. The limitation of our study is its *in vitro* character. Further *in vivo* investigation is needed to reveal the role of SF3B3 and GCH1 in ZIKV infection.

The subcellular location of host factors influences ZIKV replication. For example, intracellular translocation of HMGB1 impacts ZIKV replication (Chin et al., 2022). However, our current findings suggest that ZIKV infection does not trigger SF3B3 and GCH1 translocation between the nucleus and cytoplasm of glioma cells.

5. Conclusions

In conclusion, we document a novel regulatory mechanism of NS5 in ZIKV infection that is specifically mediated by the regulation of SF3B3 and GCH1 to modulate the innate immune response. The regulatory effect of GCH1 on ZIKV replication and IFN signalling is weaker than SF3B3. Thus, the hypothesis that SF3B3 mediates antiviral effects on ZIKV by targeting GCH1 is reasonable. These results provide a better understanding of the roles of SF3B3 and GCH1 in ZIKV infection.

Data availability

The authors confirm that the data supporting the findings of this study are available within the article.

Ethics statement

No human or animal subjects were involved in this study.

Author contributions

Tanxiu Chen: conceptualization, investigation, formal analysis, visualization, writing-original draft. Hao Yang, Penghui Liu, Moliduer Hamiti, Xintian Zhang, and Yi Xu: methodology, software. Wenqi Quan, Yong Zhang, and Bin Yin: Resources. Juemin Xi, Li Jiao, Tingfu Du, Wenhai Yu, Wei Zhou: methodology, validation, supervision. Shuaiyao Lu: funding acquisition, supervision, writing-review and editing. Xiaozhong Peng: conceptualization, funding acquisition, supervision, writing-review and editing.

Conflict of interest

The authors declare no conflict of interest.

Acknowledgements

This study was supported by the National Key R&D Project of China (2021YFC230170402), and CAMS Innovation Fund for Medical Sciences (2021-1-I2M-038).

Appendix A. Supplementary data

Supplementary data to this article can be found online at https://doi.org/10.1016/j.virs.2022.12.005.

References

Barrows, N.J., Campos, R.K., Liao, K.C., Prasanth, K.R., Soto-Acosta, R., Yeh, S.C., Schott-Lerner, G., Pompon, J., Sessions, O.M., Bradrick, S.S., Garcia-Blanco, M.A., 2018. Biochemistry and molecular Biology of flaviviruses. Chem. Rev. 118, 4448–4482.
Best, S.M., 2017. The many faces of the flavivirus NS5 protein in antagonism of type I interferon signaling. J. Virol. 91.
Chen, J., Yang, Y.F., Yang, Y., Zou, P., Chen, J., He, Y., Shui, S.L., Cui, Y.R., Bai, R., Liang, Y.J., Hu, Y., Jiang, B., Lu, L., Zhang, X., Liu, J., Xu, J., 2018. AXL promotes Zika virus infection in astrocytes by antagonizing type I interferon signalling. Nat Microbiol 3, 302–309.
Chen, K., Xiao, H., Zeng, J., Yu, G., Zhou, H., Huang, C., Yao, W., Xiao, W., Hu, J., Guan, W., Wu, L., Huang, J., Huang, Q., Xu, H., Ye, Z., 2017. Alternative splicing of EZH2 pre-mRNA by SF3B3 contributes to the tumorigenic potential of renal cancer. Clin. Cancer Res. 23, 3428–3441.
Chin, K.L., Zainal, N., Sam, S.S., Hassandarvish, P., Lani, R., Abubakar, S., 2022. Intracellular translocation of HMGB1 is important for Zika virus replication in Huh7 cells. Sci. Rep. 12, 1054.
Diamond, M.S., 2009. Mechanisms of evasion of the type I interferon antiviral response by flaviviruses. J. Interferon Cytokine Res. 29, 521–530.
Fanunza, E., Grandi, N., Quartu, M., Carletti, F., Ermellino, L., Milia, J., Corona, A., Capobianchi, M.R., Ippolito, G., Tramontano, E., 2021. INMI1 zika virus NS4B antagonizes the interferon signaling by suppressing STAT1 phosphorylation. Viruses 13.
Finci, L.I., Zhang, X., Huang, X., Zhou, Q., Tsai, J., Teng, T., Agrawal, A., Chan, B., Irwin, S., Karr, C., Cook, A., Zhu, P., Reynolds, D., Smith, P.G., Fekkes, P., Buonamici, S., Larsen, N.A., 2018. The cryo-EM structure of the SF3b spliceosome complex bound to a splicing modulator reveals a pre-mRNA substrate competitive mechanism of action. Genes Dev. 32, 309–320.
Flory, C., Chan, K.W.K., Bifani, A.M., Choy, M.M.J., Lescar, J., Ooi, E.E., Tautz, N., Vasudevan, S.G., 2021. Optimal flexibility of the linker region of Zika virus NS5 methyltransferase-polymerase is critical for virus replication. Antivir. Res. 195, 105194.
Fontaine, K.A., Leon, K.E., Khalid, M.M., Tomar, S., Jimenez-Morales, D., Dunlap, M., Kaye, J.A., Shah, P.S., Finkbeiner, S., Krogan, N.J., Ott, M., 2018. The cellular NMD pathway restricts zika virus infection and is targeted by the viral capsid protein. mBio 9, e02126-18.
Gharbi-Ayachi, A., Santhanakrishnan, S., Wong, Y.H., Chan, K.W.K., Tan, S.T., Bates, R.W., Vasudevan, S.G., El Sahili, A., Lescar, J., 2020. Non-nucleoside inhibitors of zika virus RNA-dependent RNA polymerase. J. Virol. 94, e0794-20.
Guo, M., Hui, L., Nie, Y., Tefsen, B., Wu, Y., 2021. ZIKV viral proteins and their roles in virus-host interactions. Sci. China Life Sci. 64, 709–719.
Hertzog, J., Dias Junior, A.G., Rigby, R.E., Donald, C.L., Mayer, A., Sezgin, E., Song, C., Jin, B., Hublitz, P., Eggeling, C., Kohl, A., Rehwinkel, J., 2018. Infection with a Brazilian isolate of Zika virus generates RIG-I stimulatory RNA and the viral NS5 protein blocks type I IFN induction and signaling. Eur. J. Immunol. 48, 1120–1136.
Huber, R.G., Lim, X.N., Ng, W.C., Sim, A.Y.L., Poh, H.X., Shen, Y., Lim, S.Y., Sundstrom, K.B., Sun, X., Aw, J.G., Too, H.K., Boey, P.H., Wilm, A., Chawla, T., Choy, M.M., Jiang, L., De Sessions, P.F., Loh, X.J., Alonso, S., Hibberd, M., Nagarajan, N., Ooi, E.E., Bond, P.J., Sessions, O.M., Wan, Y., 2019. Structure mapping of dengue and Zika viruses reveals functional long-range interactions. Nat. Commun. 10, 1408.
Ivashkiv, L.B., Donlin, L.T., 2014. Regulation of type I interferon responses. Nat. Rev. Immunol. 14, 36–49.
Khairallah, A., Ross, C.J., Tastan Bishop, O., 2021. GTP cyclohydrolase I as a potential drug target: new insights into its allosteric modulation via normal mode analysis. J. Chem. Inf. Model. 61, 4701–4719.
Kovanich, D., Saisawang, C., Sittipaisankul, P., Ramphan, S., Kalpongnukul, N., Somparn, P., Pisitkun, T., Smith, D.R., 2019. Analysis of the zika and Japanese encephalitis virus NS5 interactomes. J. Proteome Res. 18, 3203–3218.
Leonhard, S.E., Mandarakas, M.R., Gondim, F.a.A., Bateman, K., Ferreira, M.L.B., Cornblath, D.R., Van Doorn, P.A., Dourado, M.E., Hughes, R.a.C., Islam, B., Kusunoki, S., Pardo, C.A., Reisin, R., Sejvar, J.J., Shahrizaila, N., Soares, C., Umapathi, T., Wang, Y., Yiu, E.M., Willison, H.J., Jacobs, B.C., 2019. Diagnosis and management of Guillain-Barre syndrome in ten steps. Nat. Rev. Neurol. 15, 671–683.
Lesage, S., Chazal, M., Beauclair, G., Batalie, D., Cerboni, S., Couderc, E., Lescure, A., Del Nery, E., Tangy, F., Martin, A., Manel, N., Jouvenet, N., 2022. Discovery of genes that modulate flavivirus replication in an interferon-dependent manner. J. Mol. Biol. 434, 167277.
Li, A., Wang, W., Wang, Y., Chen, K., Xiao, F., Hu, D., Hui, L., Liu, W., Feng, Y., Li, G., Tan, Q., Liu, Y., Wu, K., Wu, J., 2020. NS5 conservative site is required for zika virus to restrict the RIG-I signaling. Front. Immunol. 11, 51.
Li, P., Jiang, H., Peng, H., Zeng, W., Zhong, Y., He, M., Xie, L., Chen, J., Guo, D., Wu, J., Li, C.M., 2021. Non-structural protein 5 of zika virus interacts with p53 in human neural progenitor cells and induces p53-mediated apoptosis. Virol. Sin. 36, 1411–1420.
Limonta, D., Hobman, T.C., 2020. Zika virus and host interactions: from the bench to the bedside and beyond. Cells 9, 2463.
Lin, S., Yang, L., Wang, S., Weng, B., Lin, M., 2020. Bioinformatics analysis of Key microRNAs and mRNAs under the hand, foot, and mouth disease virus infection. Pol. J. Microbiol. 69, 479–490.
Mahony, R., Gargan, S., Roberts, K.L., Bourke, N., Keating, S.E., Bowie, A.G., O'farrelly, C., Stevenson, N.J., 2017. A novel anti-viral role for STAT3 in IFN-alpha signalling responses. Cell. Mol. Life Sci. 74, 1755–1764.
Miao, M., Yu, F., Wang, D., Tong, Y., Yang, L., Xu, J., Qiu, Y., Zhou, X., Zhao, X., 2019. Proteomics profiling of host cell response via protein expression and phosphorylation upon dengue virus infection. Virol. Sin. 34, 549–562.
Musso, D., Gubler, D.J., 2016. Zika virus. Clin. Microbiol. Rev. 29, 487–524.
Musso, D., Ko, A.I., Baud, D., 2019. Zika virus infection - after the pandemic. N. Engl. J. Med. 381, 1444–1457.
Nan, Y., Wu, C., Zhang, Y.J., 2017. Interplay between janus kinase/signal transducer and activator of transcription signaling activated by type I interferons and viral antagonism. Front. Immunol. 8, 1758.
Ngono, A.E., Shresta, S., 2018. Immune response to dengue and zika. Annu. Rev. Immunol. 36, 279–308.
Ren, K., Sun, H., Chen, L., Chen, N., Yu, L., 2021. Myxovirus resistance protein A activates type I IFN signaling pathway to inhibit Zika virus replication. Virus Res. 306, 198534.
Roby, J.A., Esser-Nobis, K., Dewey-Verstelle, E.C., Fairgrieve, M.R., Schwerk, J., Lu, A.Y., Soveg, F.W., Hemann, E.A., Hatfield, L.D., Keller, B.C., Shapiro, A., Forero, A., Stencel-Baerenwald, J.E., Savan, R., Gale Jr., M., 2020. Flavivirus nonstructural protein NS5 dysregulates HSP90 to broadly inhibit JAK/STAT signaling. Cells 9, 899.
Sajidah, E.S., Lim, K., Wong, R.W., 2021. How SARS-CoV-2 and other viruses build an invasion route to hijack the host nucleocytoplasmic trafficking system. Cells 10, 1424.
Schilling, M., Bridgeman, A., Gray, N., Hertzog, J., Hublitz, P., Kohl, A., Rehwinkel, J., 2020. RIG-I plays a dominant role in the induction of transcriptional changes in zika virus-infected cells, which protect from virus-induced cell death. Cells 9, 1476.

Schreiber, C.A., Sakuma, T., Izumiya, Y., Holditch, S.J., Hickey, R.D., Bressin, R.K., Basu, U., Koide, K., Asokan, A., Ikeda, Y., 2015. An siRNA screen identifies the U2 snRNP spliceosome as a host restriction factor for recombinant adeno-associated viruses. PLoS Pathog. 11, e1005082.

Shah, P.S., Link, N., Jang, G.M., Sharp, P.P., Zhu, T., Swaney, D.L., Johnson, J.R., Von Dollen, J., Ramage, H.R., Satkamp, L., Newton, B., Huttenhain, R., Petit, M.J., Baum, T., Everitt, A., Laufman, O., Tassetto, M., Shales, M., Stevenson, E., Iglesias, G.N., Shokat, L., Tripathi, S., Balasubramaniam, V., Webb, L.G., Aguirre, S., Willsey, A.J., Garcia-Sastre, A., Pollard, K.S., Cherry, S., Gamarnik, A.V., Marazzi, I., Taunton, J., Fernandez-Sesma, A., Bellen, H.J., Andino, R., Krogan, N.J., 2018. Comparative flavivirus-host protein interaction mapping reveals mechanisms of dengue and zika virus pathogenesis. Cell 175, 1931–1945 e1918.

Shan, C., Xie, X., Shi, P.Y., 2018. Zika virus vaccine: progress and challenges. Cell Host Microbe 24, 12–17.

Shi, Y., Gao, G.F., 2017. Structural Biology of the zika virus. Trends Biochem. Sci. 42, 443–456.

Song, W., Zhang, H., Zhang, Y., Chen, Y., Lin, Y., Han, Y., Jiang, J., 2021. Identification and characterization of zika virus NS5 methyltransferase inhibitors. Front. Cell. Infect. Microbiol. 11, 665379.

Stegeman, R., Spreacker, P.J., Swanson, S.K., Stephenson, R., Florens, L., Washburn, M.P., Weake, V.M., 2016. The spliceosomal protein SF3B5 is a novel component of Drosophila SAGA that functions in gene expression independent of splicing. J. Mol. Biol. 428, 3632–3649.

Thurmond, S., Wang, B., Song, J., Hai, R., 2018. Suppression of type I interferon signaling by flavivirus NS5. Viruses 10, 712.

Uchida, Y., Watanabe, C., Takemae, N., Hayashi, T., Oka, T., Ito, T., Saito, T., 2012. Identification of host genes linked with the survivability of chickens infected with recombinant viruses possessing H5N1 surface antigens from a highly pathogenic avian influenza virus. J. Virol. 86, 2686–2695.

Wang, B., Thurmond, S., Hai, R., Song, J., 2018. Structure and function of Zika virus NS5 protein: perspectives for drug design. Cell. Mol. Life Sci. 75, 1723–1736.

Wei, J.L., Wu, S.Y., Yang, Y.S., Xiao, Y., Jin, X., Xu, X.E., Hu, X., Li, D.Q., Jiang, Y.Z., Shao, Z.M., 2021. GCH1 induces immunosuppression through metabolic reprogramming and Ido1 upregulation in triple-negative breast cancer. J Immunother Cancer 9.

Wei, X., Yi, X., Zhu, X.H., Jiang, D.S., 2020. Posttranslational modifications in ferroptosis. Oxid. Med. Cell. Longev. 2020, 8832043.

Wilder-Smith, A., Osman, S., 2020. Public health emergencies of international concern: a historic overview. J. Trav. Med. 27, taaa227.

Zhang, S., Zhang, J., An, Y., Zeng, X., Qin, Z., Zhao, Y., Xu, H., Liu, B., 2021. Multi-omics approaches identify SF3B3 and SIRT3 as candidate autophagic regulators and druggable targets in invasive breast carcinoma. Acta Pharm. Sin. B 11, 1227–1245.

Zhao, B., Yi, G., Du, F., Chuang, Y.C., Vaughan, R.C., Sankaran, B., Kao, C.C., Li, P., 2017. Structure and function of the Zika virus full-length NS5 protein. Nat. Commun. 8, 14762.

Zhao, Z., Tao, M., Han, W., Fan, Z., Imran, M., Cao, S., Ye, J., 2021. Nuclear localization of Zika virus NS5 contributes to suppression of type I interferon production and response. J. Gen. Virol. 102, 001376.

Zhu, S., Luo, H., Liu, H., Ha, Y., Mays, E.R., Lawrence, R.E., Winkelmann, E., Barrett, A.D., Smith, S.B., Wang, M., Wang, T., Zhang, W., 2017. p38MAPK plays a critical role in induction of a pro-inflammatory phenotype of retinal Muller cells following Zika virus infection. Antivir. Res. 145, 70–81.